

Variable Rate LPPT Based Droop Controlled Operation of Photovoltaic System for Microgrid Frequency Regulation

V. Janaki Ramaiah

A Thesis Submitted to
Indian Institute of Technology Hyderabad
In Partial Fulfillment of the Requirements for
The Degree of Master of Technology



Department of Electrical Engineering

June 2016

Declaration

I declare that this written submission represents my ideas in my own words, and where ideas or words of others have been included, I have adequately cited and referenced the original sources. I also declare that I have adhered to all principles of academic honesty and integrity and have not misrepresented or fabricated or falsified any idea/data/fact/source in my submission. I understand that any violation of the above will be a cause for disciplinary action by the Institute and can also evoke penal action from the sources that have thus not been properly cited, or from whom proper permission has not been taken when needed.



(Signature)

(V. Janaki Ramaiah)

EE14MTECH11032

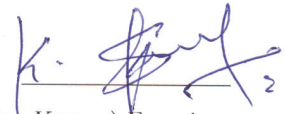
(Roll No.)

Approval Sheet


This Thesis entitled **Variable Rate LPPT Based Droop Controlled Operation of Photovoltaic System for Microgrid Frequency Regulation** by **V. Janaki Ramaiah** is approved for the degree of Master of Technology from IIT Hyderabad



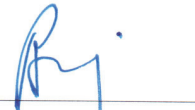
(Dr. B. Ravi Kumar) Examiner
Dept. of Electrical Engineering
IITH



(Dr. K. Siva Kumar) Examiner
Dept. of Electrical Engineering
IITH



(Dr. Vaskar Sarkar) Adviser
Dept. of Electrical Engineering
IITH



(Dr. Raja Banerjee) Chairman
Dept. of Mechanical and Aerospace Engineering
IITH

Acknowledgements

I express my deepest gratitude to my project guide **Dr. Vaskar Sarkar**, Assistant Professor, Department of Electrical Engineering, IIT Hyderabad, whose encouragement, guidance and support from the initial level to the final level enabled me to develop an understanding of the subject. It was a great honour for me to pursue my Masters under his supervision.

I am grateful to my committee members **Dr. Y. Pradeep Kumar**, **Dr. B. Ravi Kumar** and **Dr. K. Siva Kumar** for their valuable comments and suggestions. I also thank my fellow graduates from Power Electronics and Power Systems stream.

My thanks and appreciations also goes to my friends in developing the project and people who have willingly helped me.

Dedication

My Parents

Abstract

The objective of this thesis is to improve the frequency regulation of an islanded microgrid system consisting of photovoltaic (PV) system. Operating the PV system in Limited power point tracking (LPPT) mode gives provision for the application of droop control on the PV system active power, which in turn enhances the frequency regulation of the microgrid. LPPT is a control technique used for extracting the desired amount of power that may be less than the maximum available power from the PV system. Variable rate LPPT is the superior control technique among the available LPPT control techniques, which is employed in the work. The droop controller implemented in this thesis provides the required power reference command for the limited power operation of a PV system based on the deviation of bus frequency from its nominal value (50 Hz/60 Hz). A case study is presented to validate the effectiveness of the above-mentioned concept.

Contents

Declaration	ii
Approval Sheet	iii
Acknowledgements	iv
Abstract	vi
Nomenclature	vii
1 Introduction	1
2 Literature Overview	3
2.1 Photovoltaic Cell Modelling	3
2.2 Photovoltaic Array Modelling	4
2.3 Characteristics of Photovoltaic Array	5
2.4 Integration of Photovoltaic Array Unit into the Grid	6
2.5 Maximum Power Point Tracking	6
2.6 Limited Power Point Tracking	10
3 Limited Power Control of a Dual Stage Grid Connected Photovoltaic Array System	11
3.1 Structure of Dual Stage Photovoltaic Array System	11
3.1.1 DC Link Voltage Controller	11
3.1.2 Current Controller	12
3.2 Perturb and Observe based LPPT Control Schemes	13
3.2.1 Fixed Step LPPT Control	13
3.2.2 Variable Step LPPT Control	13
3.2.3 Variable Rate LPPT Control	14
3.3 Simulation Results	15
4 Frequency Regulation of an Islanded Microgrid	19
4.1 Droop Control of a PV System	19
4.2 Simulation Results	21
5 Conclusion and Future Work	26
5.1 Conclusion	26
5.2 Future Work	26

Chapter 1

Introduction

In a conventional power system, the balance between scheduled generation and actual load (plus loss) is necessary in order to maintain grid frequency at its nominal value (50 Hz in India). However, the load applied on the grid varies from time to time and is unpredictable. In order to meet the load changes, generators will have to deviate from their respective scheduled generation. In order to have proper load power sharing, the generators are operated in drooping mode. In the droop mode, the generators will raise their generation when the system frequency is less than its nominal value and vice-versa. In the conventional power system, all the generators share the real time load deviation by operating in droop mode; thus the system frequency is maintained at a decent level.

With the day to day depletion of conventional energy sources, the electricity generation from renewable energy sources such as solar, wind, tidal and so on, drawn the attention of many researchers. The easy implantation of solar panels and windmills near to the load centers and the technology advancements made in power electronics have led to the evolution of a concept called distributed generation. Integration of the distributed energy sources along with local loads is considered to be as microgrid. The microgrid can be operated either in the grid-connected mode or in the islanded mode. In the grid-connected mode, the voltage and frequency are determined by the grid and the distributed energy resources are controlled to supply only the specified amounts of active power and reactive power. In the islanded mode, the frequency and voltage are to be regulated by the distributed energy sources. So, in order to regulate the frequency and to maintain it within its limits in an islanded microgrid operation, the distributed energy sources should be operated in the drooping mode.

Easy implantation and eco-friendly generation of electricity from photovoltaic (PV) system drawn the attention of many industrialists and researchers. The mathematical modelling of PV panels is explained in [1]. Different control methods have been developed to extract the maximum available power from the PV system. Some of them are perturb and observe method, incremental conductance method, hill-climbing method, ripple correction control method and so on. The detailed comparison of all the maximum power point tracking (MPPT) control techniques is presented in [2] and [3]. MPPT operation of PV system requires additional storage for maintaining balance between generation and load. Operating PV system in MPPT mode may cause line overloading during peak power generation. To overcome this issue, a control technique is described in [4] to limit the power output from a PV system. However, here, with the selected perturbation voltage step size in perturb

and observe based limited power point tracking(LPPT) approach, there is always a conflict between response time and oscillations in power output of PV system. In the context of improving the performance of the basic LPPT control scheme, two other control schemes, namely, variable step LPPT (VSLPPT) and variable rate LPPT (VRLPPT) are developed in [5]. Operating the PV system in LPPT mode, rather than in MPPT mode, gives the provision for applying droop control on the PV system power output. This thesis, presents the effect on the frequency regulation of an islanded microgrid, by operating the PV system in drooping mode.

Organization of Thesis

Chapter 2: This chapter describes the characteristics of PV array and conventional control techniques that are used for extracting the power from PV array. Different configurations that are used for integrating the PV array to the grid is also discussed.

Chapter 3: In this chapter, perturb and observe based LPPT control techniques are explained. The performance of LPPT techniques over a dual stage grid connected PV system is studied using MATLAB/Simulink.

Chapter 4: In this chapter, the distributed sources are interconnected as an islanded microgrid system and are operated in the droop control mode. Simulation studies are performed to investigate the effectiveness of drooping operation of PV system on the microgrid frequency regulation.

Chapter 5: In this chapter, the thesis is concluded and future scope is presented.

Chapter 2

Literature Overview

This chapter describes the non-linear characteristics of the PV array, the maximum power control and the limited power control techniques used for power extraction from PV array. Moreover, different configurations used for integration of PV array with the grid is described.

2.1 Photovoltaic Cell Modelling

PV cells are the basic units of the PV array. Different equivalent circuits for modelling a PV cell can be found in the literature. They are single-diode circuit [6], [7], two-diode circuit [8], [9] and three-diode circuit [10] models. Amongst them, Single-diode circuit modelling is the most commonly used in the simulation studies due to its simplicity and accuracy. The single-diode equivalent circuit of a PV cell is shown in Fig. 2.1. The series resistance (R_s) represents the structural resistance of the PV cell. The leakage current of the p - n junction is modelled by the parallel resistance (R_p). The current-voltage equation of PV cell can be derived as given in (2.1).

$$\begin{aligned} I_c &= I_g - I_d - I_p \\ &= I_g - I_o \left(e^{\frac{\beta(V_c + R_s I_c)}{A}} \right) - \left(\frac{V_c + R_s I_c}{R_p} \right). \end{aligned} \quad (2.1)$$

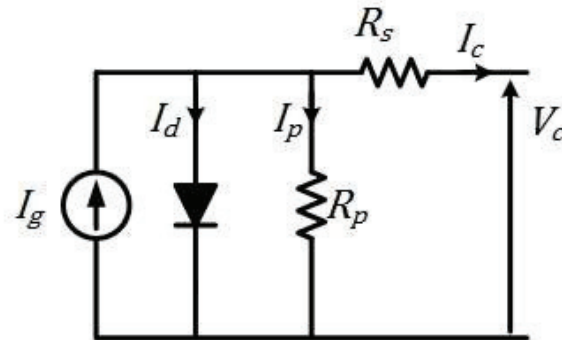


Figure 2.1: Single diode equivalent circuit of a PV cell.

Here, A is the diode ideality factor and its value is assumed to be between 1.0 and 2.5 depending on the PV device type. I_o is the diode reverse saturation current. β is the inverse thermal voltage and is defined as given in (2.2).

$$\beta = \frac{q}{KT}. \quad (2.2)$$

Here, q represents the electron charge ($1.6 \times 10^{-19}C$), K is the Boltzmann's constant ($1.38 \times 10^{-23}J/K$) and T is the $p-n$ junction temperature (Kelvin). The PV cell generated current (I_g) varies with change in irradiance (G) and temperature (T). The dependence equation of current generated by PV cell is represented as given in (2.3).

$$I_g = [I_{scr} + K_i(T - T_r)] \frac{G}{G_r}. \quad (2.3)$$

Here, I_{scr} is the short circuit current of PV cell at the standard test condition (STC). STC refers to an irradiance level of 1000 Wm^{-2} and a temperature of 25^0 C . The irradiance and temperature at STC are denoted by G_r and T_r respectively. K_i is the current temperature coefficient (A/K). The diode reverse saturation current (I_o) depends only on the temperature. In the open circuit condition, the dependence of I_o on temperature is given in (2.4).

$$I_o = \frac{I_{scr} + K_i(T - T_r)}{e^{\frac{\beta}{A}(V_{ocr} + K_v(T - T_r))} - 1}. \quad (2.4)$$

Here, V_{ocr} is the open circuit voltage at STC. K_v is the voltage temperature coefficient (V/K).

2.2 Photovoltaic Array Modelling

PV array is the series-parallel combination of PV cells. The equivalent circuit of PV cell can be extended for modelling the PV array. However, the parameters of the PV cell are to be modified by taking number of series cells (N_s) and parallel strings (N_p) into consideration. The equations (2.5)-(2.13) represents the required parameter modifications for modelling the PV array. The parameters with superscript 'a' in (2.5)-(2.13) refers to the PV array.

$$I_g^a = N_p I_g \quad (2.5)$$

$$I_o^a = N_p I_o \quad (2.6)$$

$$A^a = N_s A \quad (2.7)$$

$$K_i^a = N_p K_i \quad (2.8)$$

$$K_v^a = N_s K_v \quad (2.9)$$

$$I_{scr}^a = N_p I_{scr} \quad (2.10)$$

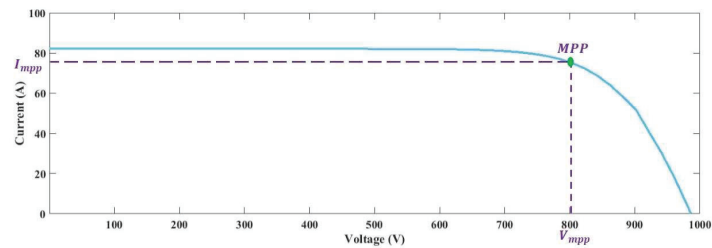
$$V_{ocr}^a = N_s V_{ocr} \quad (2.11)$$

$$R_s^a = \left(\frac{N_s}{N_p} \right) R_s \quad (2.12)$$

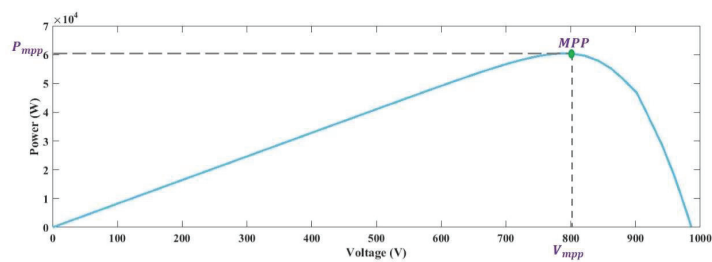
$$R_p^a = \left(\frac{N_s}{N_p} \right) R_p \quad (2.13)$$

2.3 Characteristics of Photovoltaic Array

Unlike the battery storage unit, the output voltage of the PV array depends on the load applied. With the varied terminal voltage, the power generated by the PV array also varies. The basic power vs. voltage and current vs. voltage characteristics of the considered PV array are shown in Fig. 2.2. Here, P_{mpp} refers to the maximum available power that can be extracted from PV array

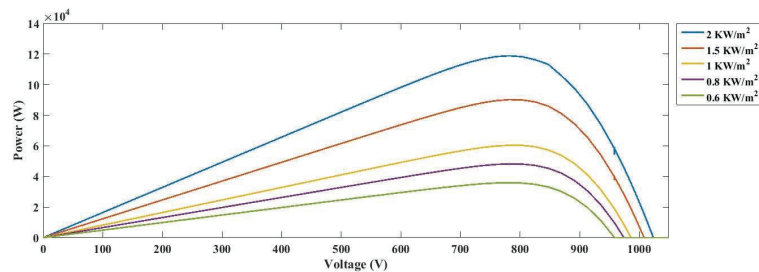


(a) Current vs. Voltage characteristics of PV array

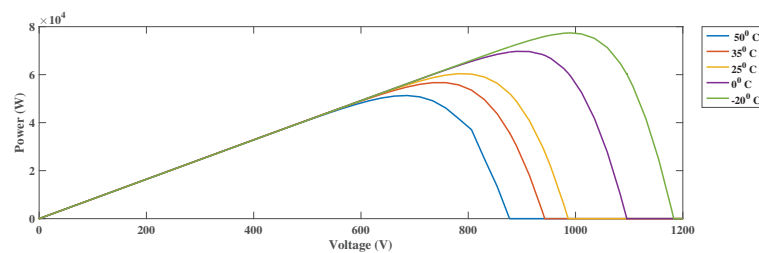


(b) Power vs. Voltage characteristics of PV array

Figure 2.2: Characteristics of PV array.



(a) Power Vs. Voltage characteristics at 25°C temperature for different irradiance levels



(b) Power Vs. Voltage characteristics at 1000 Wm^{-2} irradiance for different temperatures

Figure 2.3: Power Vs. Voltage characteristics of PV array under varying environmental conditions.

Table 2.1: Parameters of PV array

Parameter	Value
Open circuit voltage of a PV cell under STC	0.6093 V
Short circuit current of a PV cell under STC	8.21 A
PV cell current-temperature coefficient	0.00032 AK ⁻¹
PV cell voltage-temperature coefficient	-0.0027 VK ⁻¹
Diode ideality factor	1.3
Number of PV cells connected in series	1620
Number of PV strings connected in parallel	10
PV cell series resistance	0.0041 Ω
PV cell parallel resistance	7.6927 Ω
Working temperature	298.15 K
Irradiance level	1 kW ⁻²

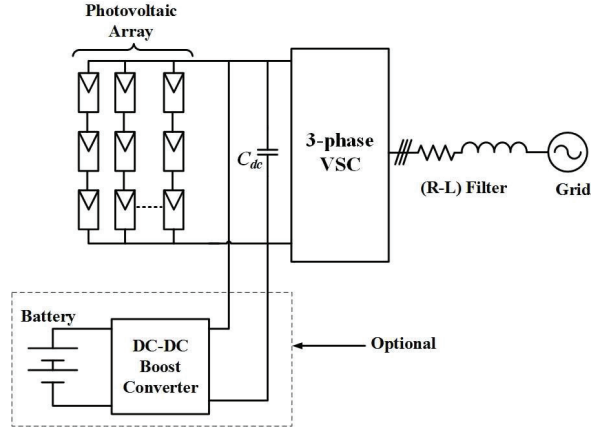
and V_{mpp} refers to the output voltage level that has to be maintained across PV array in order to extract maximum available power and I_{mpp} is the current supplied by PV array at maximum power point. It can be observed from Fig. 2.2 (b), the slope of the curve is positive on the left side of V_{mpp} , negative on the right side of V_{mpp} and zero at V_{mpp} . The parameters of the considered PV array are given in Table. 2.1. The power generated by PV array also depends on the environmental conditions and varies with the change in irradiance level and panel temperature. Fig. 2.3 describes the variation of power generated by PV array with respect to output voltage level under different irradiance and temperature levels.

2.4 Integration of Photovoltaic Array Unit into the Grid

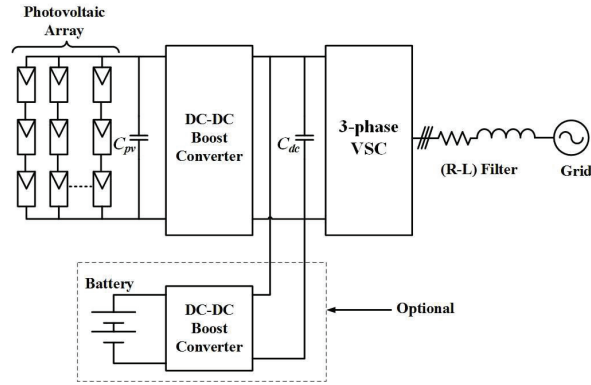
In order to integrate a PV power into the grid, power electronic interfaces are required. The configuration of PV array integration with the grid is classified based on the number of energy conversion stages used. Popularly, there are two different configurations used to integrate PV array to the grid. Those are single stage configuration and dual stage configuration and are shown in Fig. 2.4. Here, the grid represents either utility grid or microgrid. Local battery storage shown in Fig. 2.4 is optional. In the single stage conversion, the PV array is integrated to the grid using three phase voltage source converter (VSC). Here, the output power of PV array undergoes power conversion once (i.e., through three phase VSC) during its integration into the grid. Here, the MPPT/LPPT control and DC link voltage control are taken care of by three phase VSC. In the dual stage conversion, the output power of PV array undergoes power conversion twice (i.e., primarily through DC-DC converter and then through three phase VSC) during its integration into the grid. Here, the PV system shown is a non-battery back-up system. Hence, the DC link voltage control is taken care of by three phase VSC and the MPPT/LPPT control is taken care of by DC-DC converter.

2.5 Maximum Power Point Tracking

Maximum power point tracking (MPPT) is the control technique used to extract the maximum available power from the PV array. It is carried out by maintaining the output voltage of PV array near to V_{mpp} . Different MPPT control techniques came into existence such as perturb and



(a) Single stage grid connected PV system configuration



(b) Dual stage grid connected PV system configuration

Figure 2.4: Grid integrated PV system configurations.

observe (P&O) [11], [12], incremental conductance (INC) [13], hill-climbing method [14], [15], ripple correlation control (RCC) [16], [17], fractional open circuit voltage and so on. A detailed comparison of all the proposed MPPT control techniques is given in [2] and [3]. In grid connected mode, the PV system are generally operated in MPPT mode to extract the maximum available power from the PV system. However, in the islanded mode of operation, local battery storage (shown in Fig. 2.4) is required for MPPT operation of PV system. The local battery storage units store the additional power generated by PV system. In case, the power generated by PV system doesn't meet the load on the system then the difference power will be supplied by local storage units. In this section, the PV system integrated to DC grid through DC-DC converter is considered to explain the MPPT control of PV system. The schematic of MPPT control architecture of PV system integrated to DC grid is shown in the Fig. 2.5. In order to extract the maximum available power from PV array, the voltage reference generator (shown in Fig. 2.5) determines the reference voltage ($V_{pv,ref}$) that has to be maintained across PV array terminals. The duty ratio (D) of DC-DC converter is determined by applying PI control to the deviation of PV array output voltage with respect to the reference voltage generated by voltage reference generator. The block diagram of duty ratio controller is shown in Fig. 2.6. In this thesis, perturb and observe (P&O) method of MPPT control technique is considered. Here, the voltage reference for the duty ratio controller is varied in fixed steps. The MPPT control

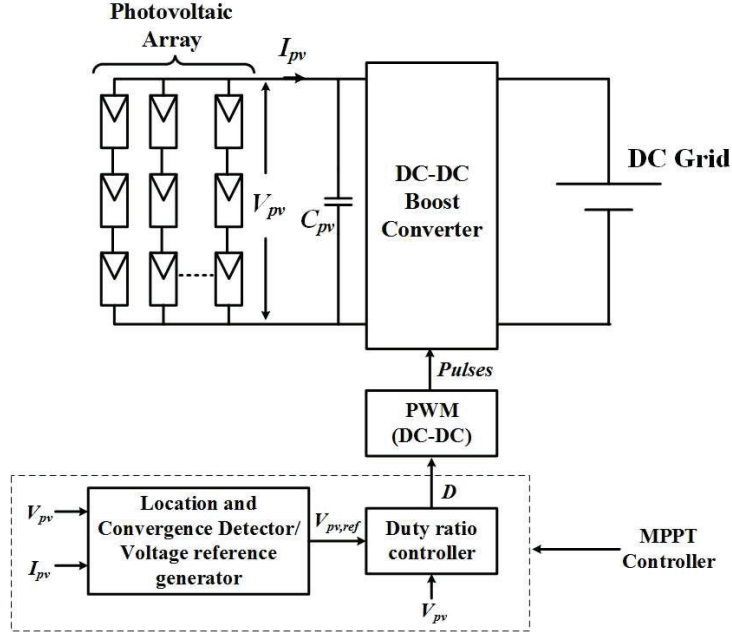


Figure 2.5: Schematic of MPPT control of DC grid integrated PV array.

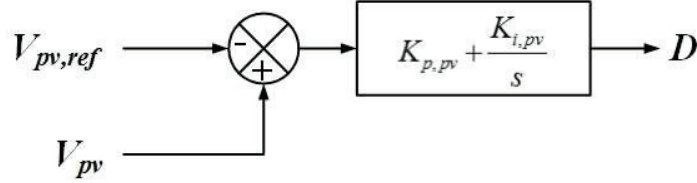


Figure 2.6: Duty ratio controller.

is governed by the following equation.

$$V_{pv,ref}[n] = V_{pv,ref}[n-1] - \sigma[n]\Delta V. \quad (2.14)$$

Here, n is the sampling time instant, ΔV is the step size for voltage correction and $\sigma[n]$ is the directionality factor. The value of directionality factor at n th sampling time instant is given in (2.15).

$$\begin{aligned} \sigma[n] &= 0 \quad \text{if } |\Gamma[n]| \leq \eta \\ &= 1 \quad \text{if } \Gamma[n] < -\eta \\ &= -1 \quad \text{if } \Gamma[n] > \eta \end{aligned} \quad (2.15)$$

Here, η represents the tolerance band for convergence at the maximum power point and is employed to avoid power oscillation. The sign of $\Gamma[n]$ for the perturb and observe (P&O) method is defined

as given in (2.16).

$$\Gamma[n] = \frac{V_{pv}[n]I_{pv}[n] - V_{pv}[n-1]I_{pv}[n-1]}{V_{pv}[n] - V_{pv}[n-1]}. \quad (2.16)$$

The sign of $\Gamma[n]$ determines the position of the present operating point on the Power Vs. Voltage curve of PV array with respect to maximum power point (MPP). The value of $\Gamma[n]$ is, positive on the left side of MPP, negative to the right of MPP and zero at MPP. The control method is described with the help of flowchart shown in Fig 2.7. This method may not be able to track true maximum power point due to the reference voltage is always varied in steps. With the high value of step change (ΔV), the reference voltage can track V_{mpp} at a faster rate. However, the power oscillations at steady state will be more with a high value of step change (ΔV). Moreover, the power oscillations at steady state can be reduced with a lesser value of step change (ΔV) but it will take more time for reference voltage to reach V_{mpp} .

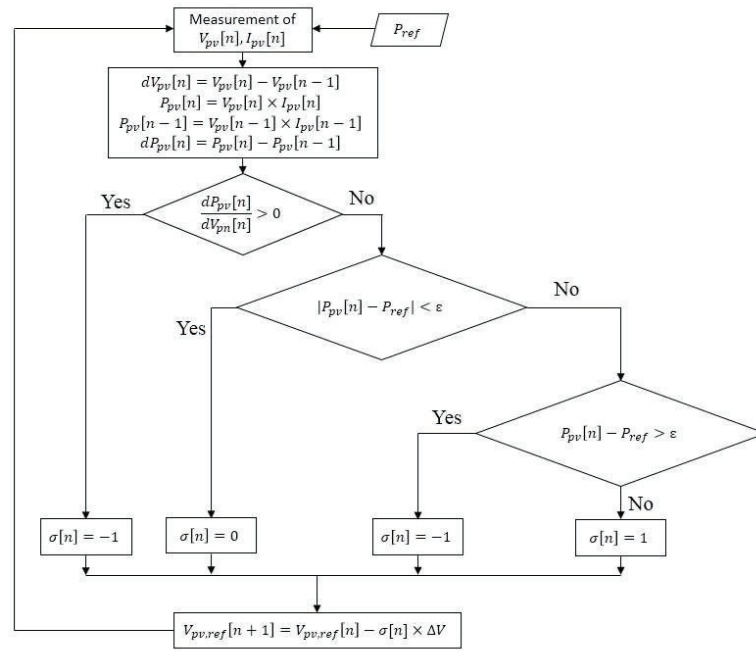


Figure 2.7: Flowchart of Perturb and Observe (P&O) method for MPPT control technique.

Disadvantages of Maximum Power Point Tracking

Even though the PV array units are effectively utilised with maximum power point control technique, there are some disadvantages with operating PV array units in MPPT mode and are given as below

1. In islanded mode, the coordinated battery storage or controllable auxillary load units are required in order to maintain generation and load balance during MPPT operation of PV system.
2. In grid connected mode, the MPPT operation of PV system may cause line overloading. The MPPT control may even degrade the system frequency profile with high penetration level of PV power.

3. The inverter life will be degraded with randomly varying PV power output (due to change in environmental conditions).

4. The high rating inverter (usually, more than the rating of the PV system) is installed for PV system operating in MPPT mode. Moreover, the inverter rating is not effectively utilized as the PV power output varies from time to time.

These disadvantages can be taken off by having coordinated energy storage, auxiliary load units to burn the excess power or by grid expansion. These approaches require more cost and even occupy more space.

2.6 Limited Power Point Tracking

Limited power point tracking (LPPT) is the control technique which helps in extracting the desired amount of power, which may be less than maximum available power, from the PV array. This approach overcomes the disadvantages of MPPT and is effective in terms of economy and occupies less space as there is no need of coordinated storage or auxiliary load units. This method helps in extracting the desired amount of power as given by the reference power command. If the given reference power is less than maximum available power then the implemented control technique tracks the reference power. Otherwise, it will track the maximum power. For every given reference power level (P_{pv}), less than maximum power point, there are two possible operating points (A & B) as shown in Fig. 2.8. The operating voltage at point B is more than operating voltage at point A . For the same power reference level, the current delivered by PV array will be less with a high value of terminal voltage. Moreover, the power loss in the PV system will be less with the less amount of current. Hence, the operating point B (with high value of terminal voltage) is preferred over operating point A (with low value of terminal voltage).

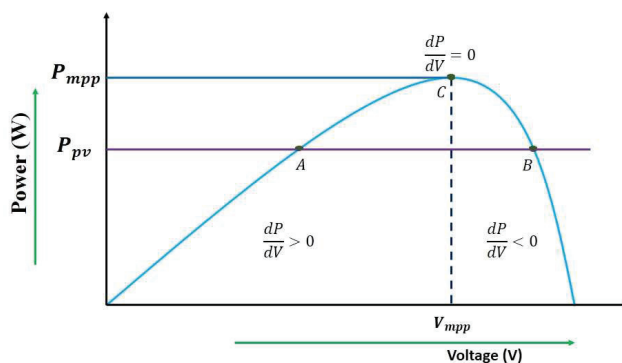


Figure 2.8: Power vs. Voltage characteristics of PV array.

Chapter 3

Limited Power Control of a Dual Stage Grid Connected Photovoltaic Array System

In this chapter, the different LPPT control schemes are investigated for limited power control operation of the dual stage grid connected PV system.

3.1 Structure of Dual Stage Photovoltaic Array System

The schematic of the basic LPPT control architecture of a dual stage PV system integrated into the grid is shown in Fig. 3.1. Here, the reference voltage across DC link capacitance (C_{dc}) is kept constant. The DC-AC converter helps to control the DC link voltage to the reference value through an outer-loop DC link voltage controller and inner-loop current controller [18]. Here, the DC link voltage controller and current controllers are implemented in dqo domain rather than in abc domain. Here, Park's transformation is used for converting the abc quantities to dqo quantities and is given in (3.1). The LPPT control is taken care of by the DC-DC converter (i.e., the output voltage of PV array is regulated by DC-DC converter). Here, perturb and observe based LPPT control is implemented for extracting desired amount of power from PV array.

$$\begin{bmatrix} f_d \\ f_q \\ f_o \end{bmatrix} = \frac{2}{3} \begin{bmatrix} \cos(\omega t) & \cos(\omega t - \frac{2\pi}{3}) & \cos(\omega t + \frac{2\pi}{3}) \\ -\sin(\omega t) & -\sin(\omega t - \frac{2\pi}{3}) & -\sin(\omega t + \frac{2\pi}{3}) \\ \frac{1}{2} & \frac{1}{2} & \frac{1}{2} \end{bmatrix} \begin{bmatrix} f_a \\ f_b \\ f_c \end{bmatrix} \quad (3.1)$$

3.1.1 DC Link Voltage Controller

The DC link voltage controller is implemented to maintain the voltage across the DC link capacitance (C_{dc}), V_{dc} , at a value given by reference voltage ($V_{dc,ref}$). The block diagram of DC link voltage controller is shown in Fig. 3.2. Here, the value of $V_{dc,ref}$ is constant and is normally maintained at a value of 1.5 times the open circuit voltage of PV array under STC. The DC link voltage

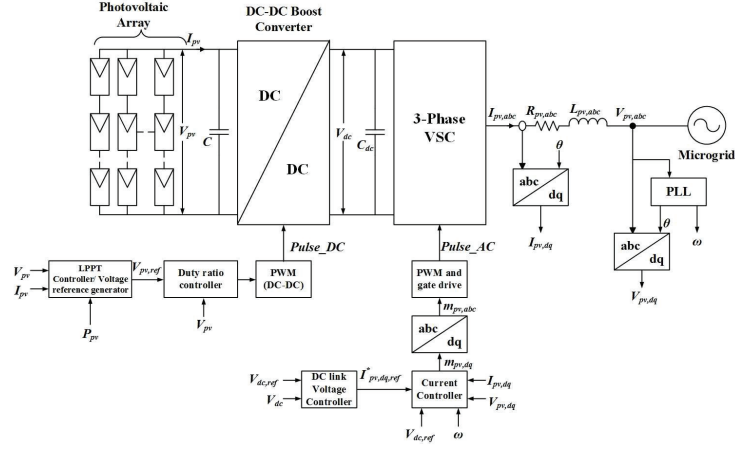


Figure 3.1: Schematic of dual-stage PV system integrated to grid.

controller produces the d -component of current reference command given to the current controller. The q -component is kept zero, to operate VSC at unity power factor.

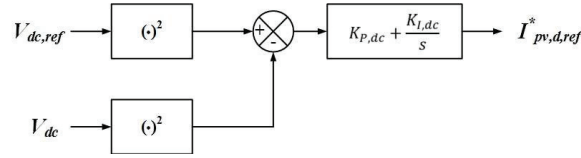


Figure 3.2: Schematic of DC link voltage controller.

3.1.2 Current Controller

The main purpose of current controller is to regulate the d and q components of filter currents ($I_{pv,dq}$) to the reference value of currents ($I_{pv,dq,ref}^*$). The block diagram of current controller is shown in Fig. 3.3.

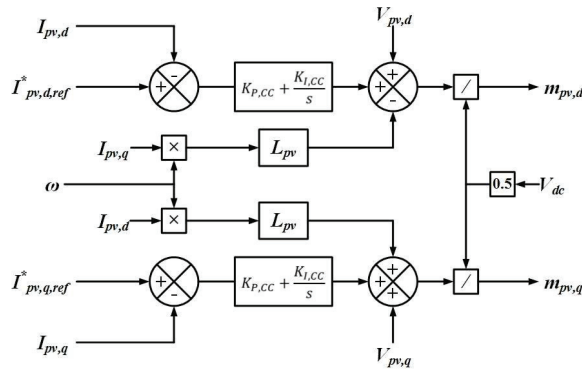


Figure 3.3: Schematic of current controller.

3.2 Perturb and Observe based LPPT Control Schemes

LPPT is the control technique used to extract the desired amount of power from PV system. The amount of power required is specified through a reference power command that, in principle, should not be no higher than the maximum available power from the PV system. However, when the reference power level is more than the maximum available power then the control shifts to maximum power point tracking mode. Three different LPPT control schemes are proposed in literature based on perturb and observe principle. Those are described as below.

3.2.1 Fixed Step LPPT Control

This is the conventional LPPT technique and here, the voltage reference for the duty ratio controller is varied in fixed steps. The fixed step LPPT (FSLPPT) control is governed by the following equation.

$$V_{pv,ref}[n] = V_{pv,ref}[n-1] - \sigma[n]\Delta V. \quad (3.2)$$

Here, n is the sampling time instant, ΔV is the step size for voltage correction and $\sigma[n]$ is the directionality factor. The value of directionality factor at n th sampling time instant is given in (3.3).

$$\begin{aligned} \sigma[n] &= 1 \quad \text{if } \Gamma[n] \leq 0 \quad \text{and } P_{pv}[n] - P_{ref} < -\varepsilon \\ &= 0 \quad \text{if } \Gamma[n] \leq 0 \quad \text{and } |P_{pv}[n] - P_{ref}| \leq \varepsilon \\ &= -1 \quad \text{Otherwise.} \end{aligned} \quad (3.3)$$

Here, ε represents the tolerance band for convergence at reference power point and is employed to avoid power oscillation. The sign of $\Gamma[n]$ for the perturb and observe (P&O) method is defined as given in (3.4).

$$\Gamma[n] = \frac{V_{pv}[n]I_{pv}[n] - V_{pv}[n-1]I_{pv}[n-1]}{V_{pv}[n] - V_{pv}[n-1]}. \quad (3.4)$$

The sign of $\Gamma[n]$ determines the position of the present operating point on the Power Vs. Voltage curve of PV array with respect to maximum power point (MPP). The value of $\Gamma[n]$ is, positive on the left side of MPP, negative to the right of MPP and zero at MPP. In this LPPT control scheme, the voltage is varied with fixed perturbation step size (ΔV) depending on the position of the present operating point with respect to MPP. Hence, this LPPT control scheme is considered to be as FSLPPT. In this control scheme, with the high value of step size (ΔV), the response time will be less and power oscillations at steady state will be more. However, with the less value of step size (ΔV), the response time will be more and power oscillations will be less. Hence, with this FSLPPT control scheme, there is always a conflict between response time and power oscillations.

3.2.2 Variable Step LPPT Control

In this control scheme, the perturbation step size is dynamically adjusted to overcome the conflict between response time and power oscillations. This scheme resembles variable step MPPT [19]. The perturbation step size is varied based on the location of the present operating point with respect to

MPP and the deviation of the power level at the present operating point from the reference power. In this control scheme, the dynamics of reference voltage generator is defined as given in (3.5).

$$V_{pv,ref}[n] = V_{pv,ref}[n-1] - \sigma[n]\alpha[n]\Delta V. \quad (3.5)$$

Here, $\sigma[n]$ and ΔV , serve the same as explained for FSLPPT. The dynamic adjustment of perturbation step size is carried out by $\alpha[n]$. As we prefer the operating point on the right-hand side of V_{mpp} , for a reference power level below the maximum power level, there is no need to vary the perturbation step size if the operating point is on the left-hand side of MPP. Hence, the perturbation step size is dynamically adjusted only on the right-hand side of MPP. The value of α , step adjustment factor, at the n th sampling time instant is defined as given in (3.6).

$$\begin{aligned} \alpha[n] &= 1 \quad \text{if } \Gamma[n] > 0 \\ &= \min\{1, \gamma|P_{pv}[n] - P_{ref}|\} \quad \text{if } \Gamma[n] \leq 0. \end{aligned} \quad (3.6)$$

Here, γ is the constant of proportionality for step adjustment and is to be tuned based upon the LPPT operation. To minimise the power oscillations during MPPT mode of operation (in the case of reference power more than the maximum available power), a power scarcity indicator (Φ) is determined and its value at n th sampling time instant is defined as given in (3.7).

$$\begin{aligned} \Phi[n] &= 0 \quad \text{if } |\Gamma[n]| \leq \epsilon \quad \text{and } P_{pv}[n] \leq P_{ref} \\ &= 1 \quad \text{Otherwise.} \end{aligned} \quad (3.7)$$

Here, ϵ determines the tolerance band for convergence of slope at maximum power point. The convergence criterion defined for VSLPPT around the reference power level is given in (3.8).

$$\sigma[n] = 0 \quad \text{if } \Phi[n] = 0 \quad \text{or } |P_{pv}[n] - P_{ref}| \leq \mu P_{ref}. \quad (3.8)$$

Here, μ is the constant of proportionality tuned for convergence at reference power level.

3.2.3 Variable Rate LPPT Control

The control performance of VSLPPT can be further improved by reducing the perturbation step size (ΔV) and increasing the sampling frequency of the voltage reference generator. However, due to the presence of transients in DC-DC converter, the location detection of a steady operating point corresponding to the present reference voltage may be incorrect with a high sampling frequency. Hence, a control scheme was developed [5] by separating the location and convergence detection module from the voltage reference generator. In this control scheme, the location and convergence detector is operated at a sampling frequency as that of conventional LPPT control scheme. However, the sampling frequency of reference voltage generator is made infinitely high and is considered to be as continuous time system and hence the control scheme is termed as variable rate LPPT (VRLPPT). The dynamics of voltage reference generator in VRLPPT is determined as given in (3.9).

$$V_{pv,ref}(t) = V_{pv,ref}(0) - \int_0^t \delta\beta(\tau) d\tau. \quad (3.9)$$

Here, the voltage variation rate is dynamically adjusted instead of the voltage perturbation step size (ΔV). Here, the parameter δ is the base magnitude of voltage variation rate. The value of β is defined as given in (3.10).

$$\begin{aligned}\beta(t) &= 0 \quad \text{if } \Phi(t) = 0 \\ &= -1 \quad \text{if } \varphi(t) = 1 \quad \text{and } \Phi(t) = 1 \\ &= \min\{1, \gamma|P_{pv} - P_{ref}|\} \quad \text{if } \varphi(t) = 0 \quad \text{and } \Phi(t) = 1\end{aligned}\tag{3.10}$$

Here, Φ represents the power scarcity indicator and is similar to that of defined in VSLPPT control scheme and its value at n th sampling time instant is given in (3.7). Here, φ refers to the location detection of operating point with respect to maximum power point and its value at n th sampling time instant is defined as given in (3.11).

$$\begin{aligned}\varphi[n] &= 0 \quad \text{if } \Gamma[n] \leq 0 \\ &= 1 \quad \text{if } \Gamma[n] > 0.\end{aligned}\tag{3.11}$$

The values of $\Phi(t)$ and $\varphi(t)$ are respectively determined by $\Phi[n]$ and $\varphi[n]$ during the interval $nT_s \leq t < (n+1)T_s$. Here, T_s represents the sampling time interval of location and convergence detector. In this thesis, VRLPPT control scheme is considered for LPPT operation of PV system as it is the superior control scheme and it helps in achieving effective power tracking [5].

3.3 Simulation Results

The effectiveness of the three different LPPT control techniques (FSLPPT, VSLPPT and VRLPPT) is investigated over dual stage grid-connected PV system using MATLAB/Simulink. The parameters of PV array given in Table. 2.1 are considered here for simulation. However, here, the panel temperature is considered to be maintained at a temperature of 35⁰ C. The boost converter parameters of the system considered are given in Table. 3.1. Here, the PV system is considered to be connected to an infinite bus. Hence, filter capacitor is not considered. The other AC side filter parameters are given in Table. 3.2. The LPPT controller parameters are given in Table. 3.3. The tuning parameters of PI control block employed in the duty ratio controller, DC link voltage controller and current controller are also given in Table. 3.3. For the first 4 seconds, an irradiance level of 1 KWm⁻² is maintained and then is reduced to 0.6 KWm⁻². The red coloured dashed line in the Fig. 3.4 represents the reference power command (P_{pv}) and is varied in steps to investigate the effectiveness of power tracking using three different LPPT control techniques. In Fig. 3.4, it can be observed that during the intervals (0-2)s and (6-8)s, the system considered is operating in the MPPT mode as the maximum available power is less than the reference power level. The system is operating in LPPT mode during the interval (2-6)s. From the results shown in Fig. 3.4, it can be observed that the FSLPPT and VSLPPT methods resulting in slow response time when operation is switched from MPPT mode to LPPT mode and from LPPT mode to MPPT mode. The VRLPPT method provides faster response to the reference power command variation compared to the FSLPPT and VSLPPT methods. In addition, the power oscillation is also less in the VRLPPT method. Hence, VRLPPT control technique is considered as the superior technique for effective tracking of power.

Table 3.1: Boost converter parameters

Parameter	Value
Inductance (L)	1 mH
Input capacitance of boost converter (C)	1.5 mF
DC link capacitance (C_{dc})	1.5 mF
Switching frequency	2 KHz
DC grid voltage (V_{dc})	1500 V

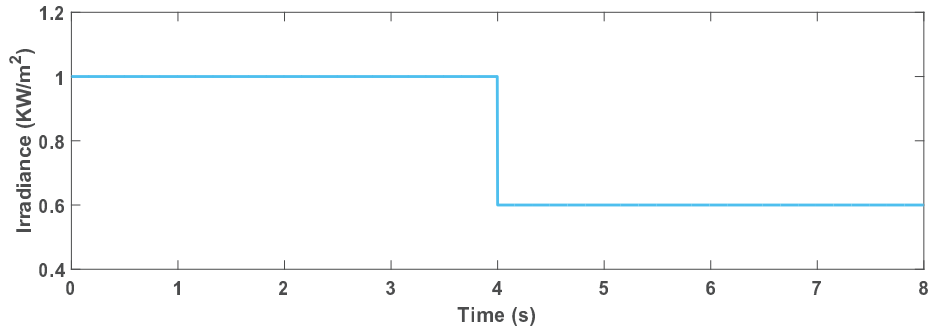
Table 3.2: AC side filter parameters

Parameter	Value
$R_{pv,abc}$	0.295 Ω
$L_{pv,abc}$	6.71 mH

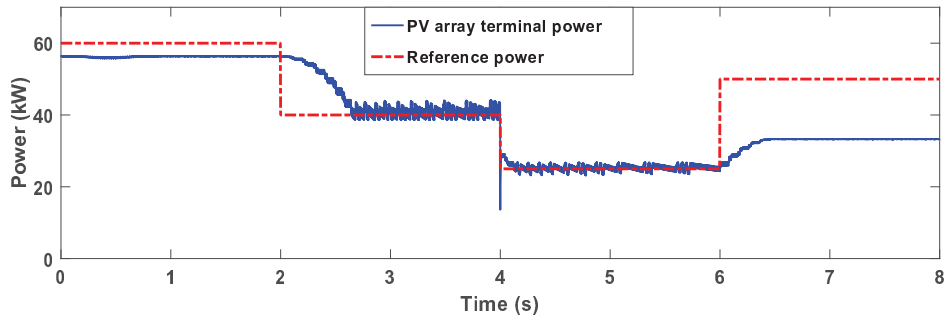
Table 3.3: LPPT controller parameters

Parameter	Value
Sampling time (T_s)	20 ms
Voltage step size (ΔV)	10 V
η	10 A
ε	600 W
γ (VSLPPT)	0.0004 W^{-1}
γ (VRLPPT)	0.002 W^{-1}
δ	300 Vs^{-1}
$K_{p,pv}$	-0.0006 V^{-1}
$K_{i,pv}$	-0.0006 $\text{V}^{-1}\text{s}^{-1}$
$K_{p,dc}$	-0.01 AV^{-2}
$K_{i,dc}$	-0.008 $\text{AV}^{-2}\text{s}^{-1}$
$K_{P,CC}$	6.71 Ω
$K_{I,CC}$	295 Ωs^{-1}

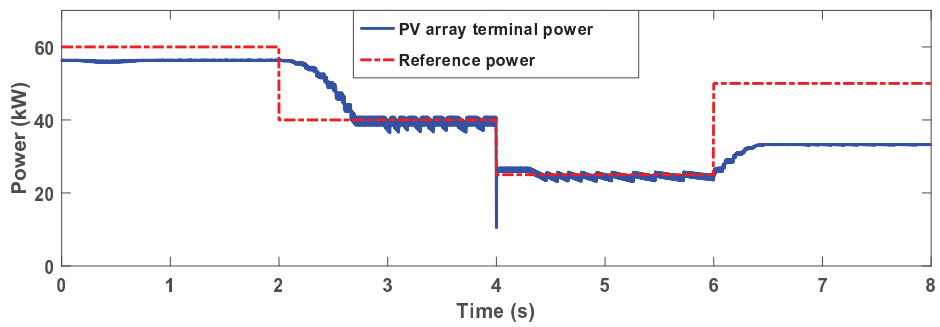
The power injected by the dual stage PV system into the grid using three different LPPT control techniques is shown in Fig. 3.5.



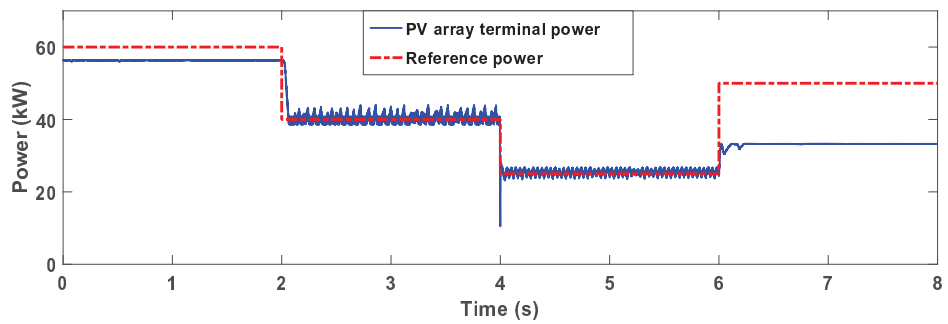
(a) Irradiance in KW/m²



(b) Power tracking using FSLPPT technique

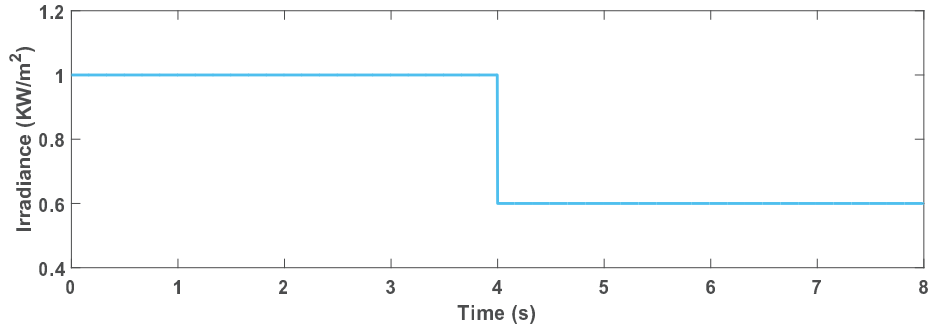


(c) Power tracking using VSLPPT technique

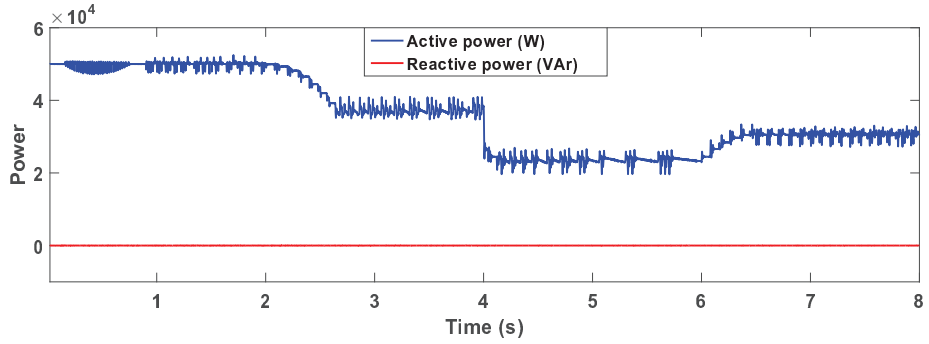


(d) Power tracking using VRLPPT technique

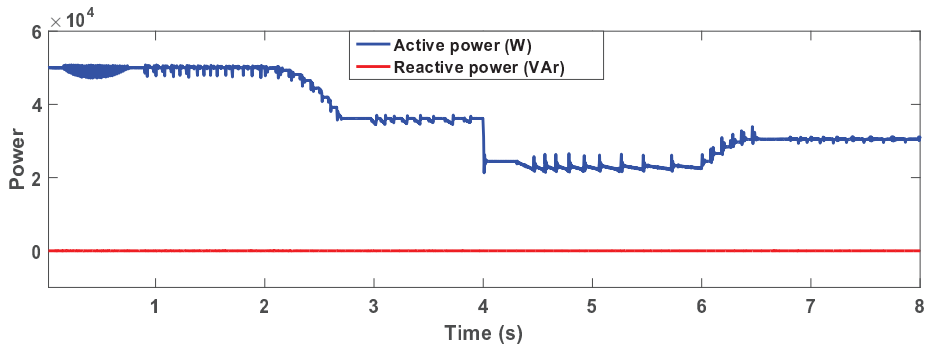
Figure 3.4: Simulation results of PV array terminal power for different LPPT techniques.



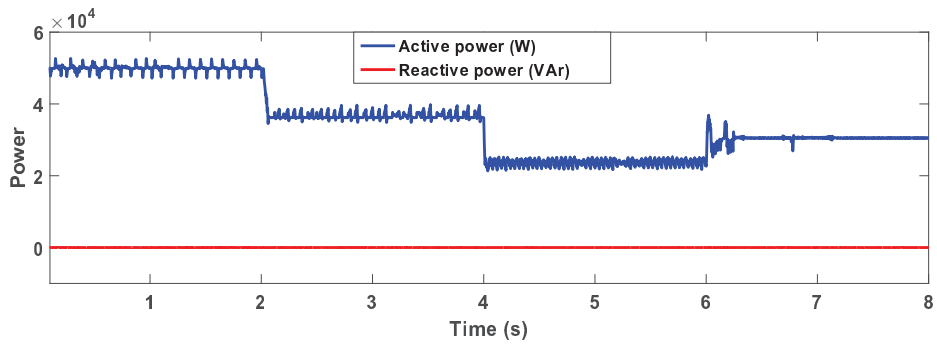
(a) Irradiance in KW/m²



(b) FSLPPT technique



(c) VSLPPT technique



(d) VRLPPT technique

Figure 3.5: Simulation results of PV system power injected into the grid using different LPPT techniques.

Chapter 4

Frequency Regulation of an Islanded Microgrid

The distributed energy sources are integrated along with loads to form a microgrid. The microgrid can be operated either in the grid-connected mode or in an islanded mode. In grid connected mode, the inertia of rotating conventional generators will take care of the frequency regulation. Other methods like electricity storage and dedicated demand response are also practiced to regulate the grid frequency [20]. During grid-connected mode, the voltage and frequency are determined by the grid and the distributed energy resources are controlled to supply only the specified amounts of active power and reactive power. In the islanded mode, the frequency and voltage are to be regulated by the distributed energy sources. So, in order to regulate the frequency and to maintain it within its limits in an islanded microgrid operation, the distributed energy sources present in the microgrid should be operated in the drooping mode. Till date, droop control could be performed only for the storage systems or for the storage backed PV system. In this thesis, the droop controller is developed for the non-battery backed PV system. Droop control of non-battery backed PV system power is possible only when it is operated in LPPT mode. In this chapter, the variable rate LPPT control scheme is considered as it helps in achieving effective power tracking compared to other LPPT techniques.

4.1 Droop Control of a PV System

Droop control operation of distributed energy sources in a microgrid enables to share its load power under normal operating conditions and any further change in load power will be compensated by the distributed energy sources. The control architecture for islanded operation of battery storage system is explained in [21], [22]. Here, the battery storage system is operated in P - ω droop control mode. The droop control implemented for battery storage system can be represented in equation form as given in (4.1).

$$\omega_{bat} = \omega_{nom} + m_{\omega}(P_{bat,ref} - P_{bat}). \quad (4.1)$$

Here, ω_{nom} is the nominal value of grid frequency (rad/sec), $P_{bat,ref}$ is the power reference set point of the battery. P_{bat} is the battery system power output. The droop control coefficient (m_ω) is tuned according to the battery storage power level and accepted deviation in grid frequency. The schematic of droop control operation of battery storage system is shown in Fig. 4.1. The current

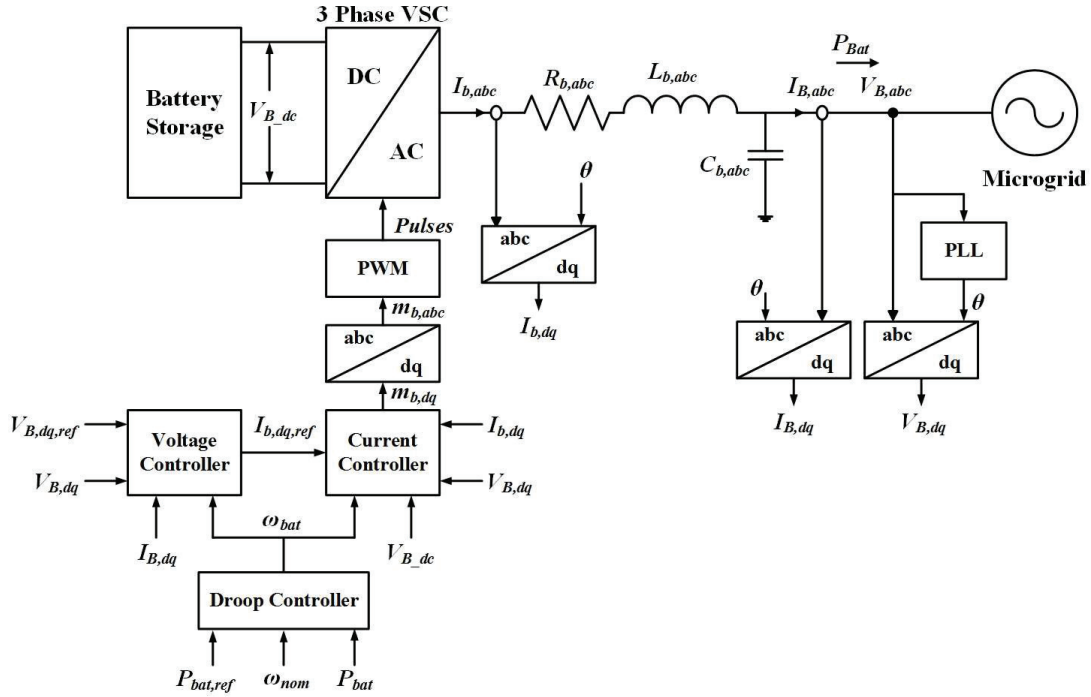


Figure 4.1: Schematic of droop control operation of a battery storage system.

controller shown in Fig. 4.1 is similar to that of explained in Section 3.1.2. The voltage controller is implemented in order to control the voltage across the filter capacitor ($C_{b,abc}$). The voltage controller generates the reference current signals ($I_{b,dq,ref}$) and is fed to the current controller. The voltage controller is implemented in dqo domain and is shown in Fig. 4.2.

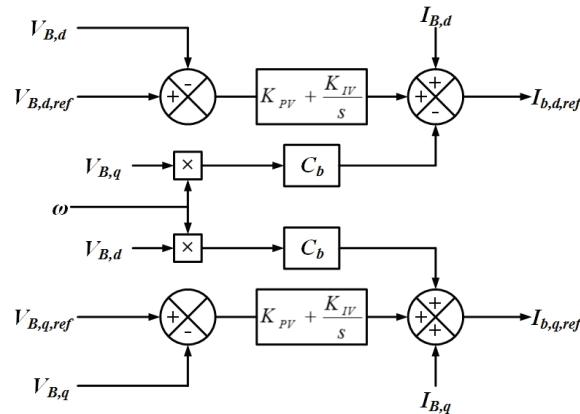


Figure 4.2: Schematic of voltage controller.

The PV system is operated in ω - P droop control mode, generating the required power reference command for LPPT operation of PV system by calculating the deviation of measured bus frequency from its nominal value. The droop control implemented for PV system is represented as given in (4.2).

$$P_{pv} = P_{pv,ref} + m_P(\omega_{nom} - \omega). \quad (4.2)$$

Here, ω is the bus frequency (rad/sec) measured by phase locked loop (PLL), $P_{pv,ref}$ is the power reference set point of the PV system droop controller, P_{pv} is the reference power command given to the LPPT controller block of PV system. The droop control coefficient (m_P) is tuned according to the PV system power level and accepted deviation in system frequency. The schematic of droop based LPPT operation of dual stage PV system is shown in Fig. 4.3.

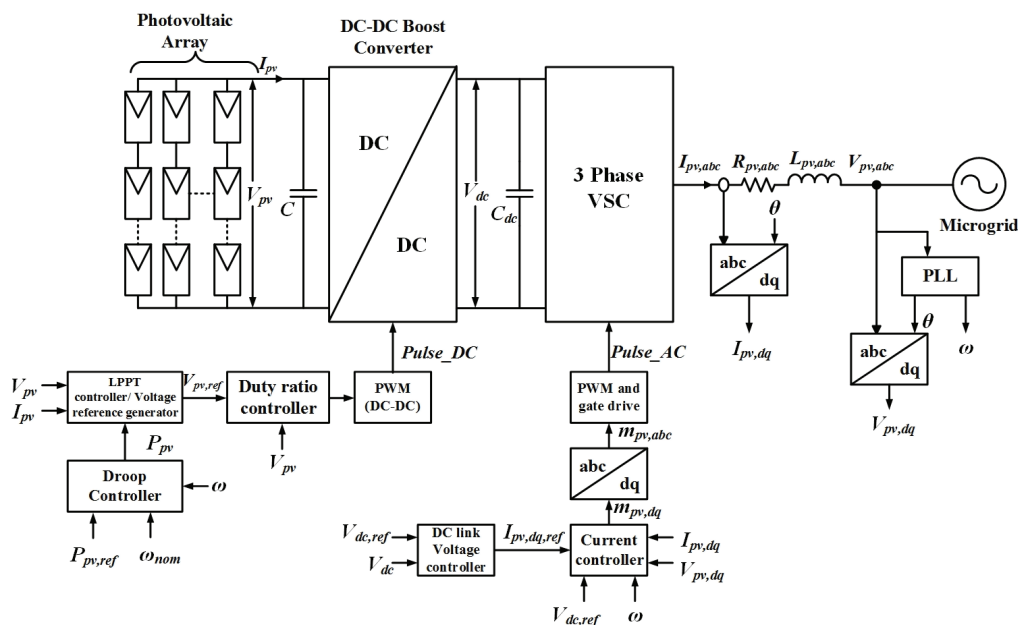


Figure 4.3: Schematic of control architecture for LPPT based droop control operation of PV system.

4.2 Simulation Results

The effect of droop based VRLPPT control operation of PV system on frequency regulation of an islanded microgrid is investigated using MATLAB/Simulink. In this paper, a battery storage system and two PV systems are considered to be interconnected as a single bus islanded microgrid system along with a balanced three phase starconnected varying resistive load and its schematic is shown in Fig. 4.4. The parameters of dual-stage PV system considered for the simulation are given in Table. 2.1, Table. 3.1, Table 3.2 and Table. 3.3. However, here, two different PV systems are considered with different series-parallel configuration of PV cells and are given in Table. 4.1. The maximum power that can be delivered by the considered PV-1 and PV-2 systems are 50 kW and 35 kW, respectively. Battery storage system parameters are given in Table. 4.2. The implemented droop

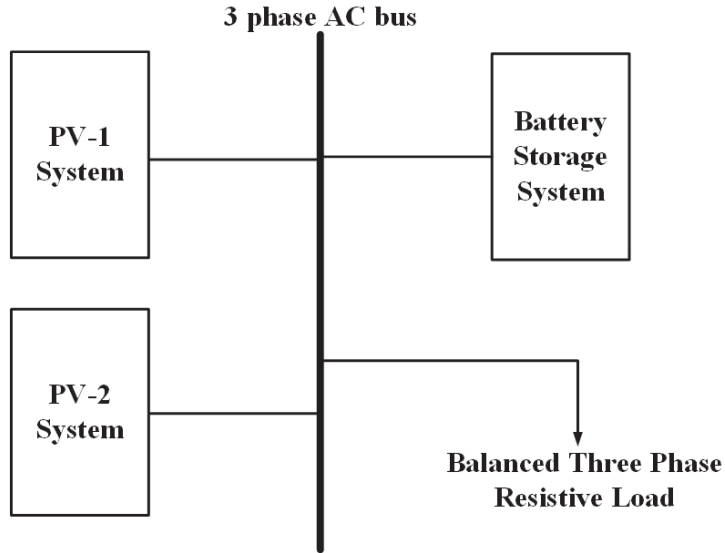


Figure 4.4: Schematic of single bus islanded microgrid.

control parameters and the nominal values of AC bus parameters are given in Table. 4.3. Here, two different cases are considered to investigate the effect on frequency regulation. In the first case, the two PV systems are operated in MPPT mode and as they always delivers maximum available power into the microgrid, battery storage system alone is operated in droop control mode. In the second case, droop control is applied to all the battery storage and PV systems by operating the PV systems under the VRLPPT control. In both the cases, the considered system is initialized to their respective nominal values. A balanced three phase star-connected resistive load of $0.7315 \omega/ph$ is applied on the integrated bus. The Load resistance is changed to $0.8736 \omega/ph$ and is maintained from 2 to 4 sec. The load resistance is again changed to $0.7735 \omega/ph$ at 4 sec. The total time considered for simulation is 6 sec. The observed results are shown in Fig. 4.5 and 4.6. From the results, it can be observed that the deviation of frequency from its nominal value is less in the case of both the PV systems and battery storage system operating in droop control mode compared to the battery storage system alone is operating in drooping mode.

Table 4.1: PV system parameters

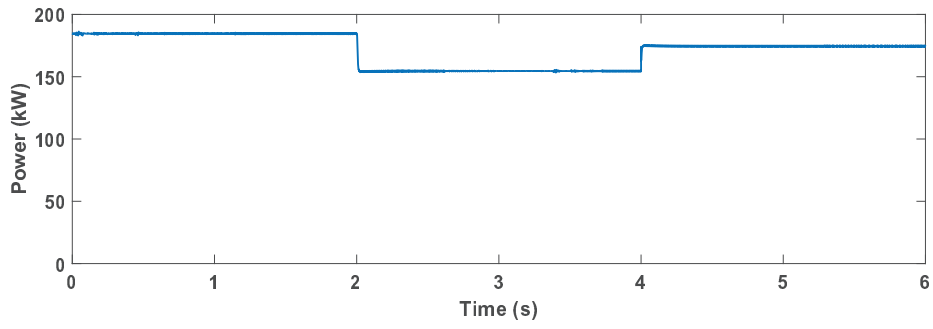
Parameter	Value
Number of cells connected in series of PV-1 system	1620
Number of strings connected in parallel of PV-1 system	10
Number of cells connected in series of PV-2 system	1080
Number of strings connected in parallel of PV-2 system	10
DC link voltage of PV-1 system	1500 V
DC link voltage of PV-2 system	1000 V

Table 4.2: Battery system parameters

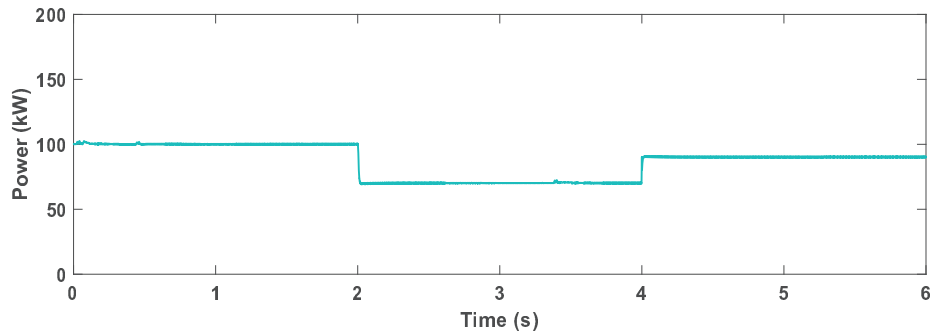
Parameter	Value
$R_{b,abc}$	0.295 Ω
$L_{b,abc}$	6.71 mH
$C_{b,abc}$	2 mF
K_{PV}	1.03294 A
K_{IV}	8.45834 As^{-1}
K_{PC}	6.71 V
K_{IC}	295 Vs^{-1}

Table 4.3: Nominal values of AC bus parameters and droop control parameters

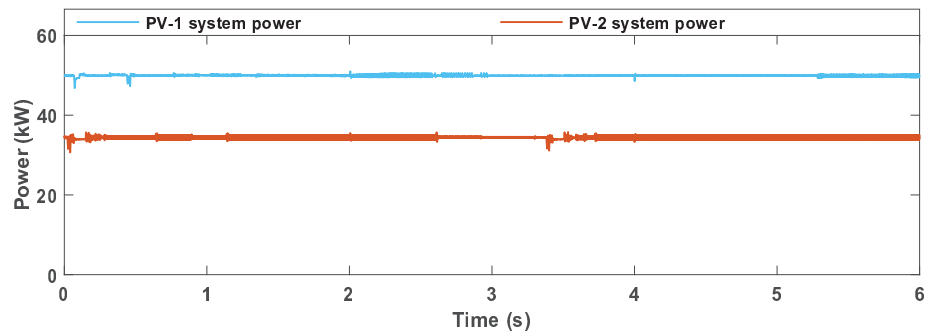
Parameter	Value
Nominal value of bus frequency (ω_{nom})	100 π rad.s^{-1}
Nominal value of bus voltage (L-N)	300 V (Peak)
Power reference set point of the battery ($P_{bat,ref}$)	100 kW
Power reference set point of the PV-1 system ($P_{pv1,ref}$)	56.25 kW
Power reference set point of the PV-2 system ($P_{pv2,ref}$)	37.58 kW
m_{ω}	2.513274 $\times 10^{-5}$ $\text{rad.s}^{-1}.\text{W}^{-1}$
m_{p1}	3.978874 $\times 10^4$ $\text{W.rad}^{-1}.\text{s}$
m_{p2}	2.7486058 $\times 10^4$ $\text{W.rad}^{-1}.\text{s}$



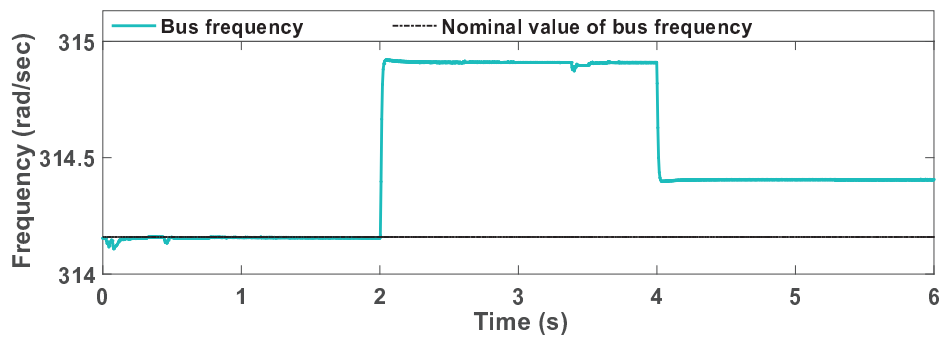
(a) Load power



(b) Battery power



(c) PV systems power



(d) Frequency in rad/sec

Figure 4.5: Power sharing and frequency profile for the MPPT operation of PV systems.

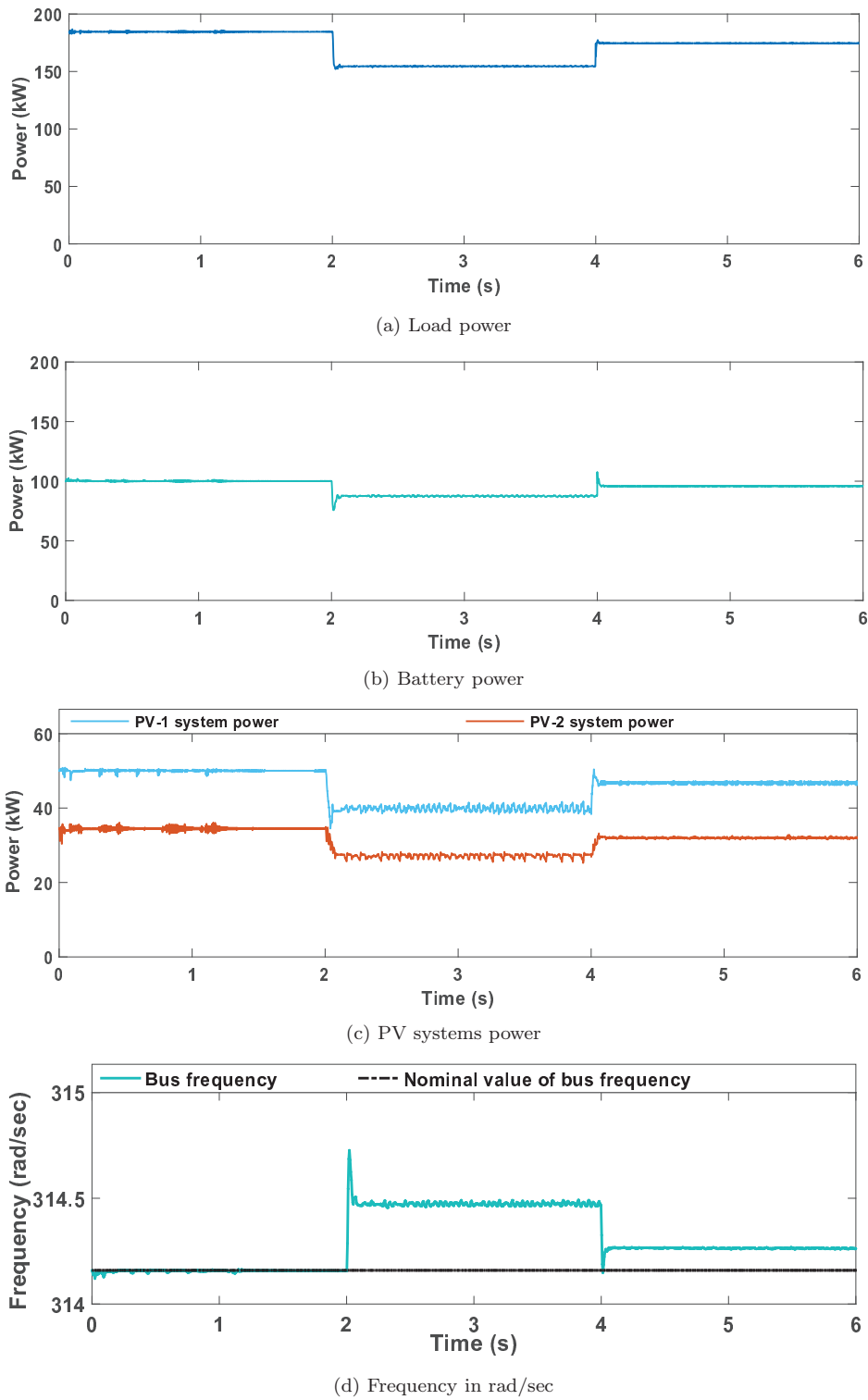


Figure 4.6: Power sharing and frequency profile for the droop controlled LPPT operation of PV systems.

Chapter 5

Conclusion and Future Work

5.1 Conclusion

The objective of the thesis is to regulate the frequency of an islanded microgrid system by operating all the available distributed energy sources in the droop control mode. Here, the droop control of the PV system power output is considered as of interest in regulating the grid frequency. Till date, droop control could be performed only for the storage system or for the battery backed PV system. Here, a droop controller for the non-battery backed PV system is developed. In this thesis, a battery storage system and two non-battery backed PV systems are integrated as the islanded microgrid system and are operated in drooping mode. The implemented drooping operation of the PV systems is different from the drooping operation of the battery storage system. The droop controller used for the storage system generates a frequency command from the power measurement, which is fed to the VSC control system. On the other hand, the droop controller used for the PV system generates a power command from the frequency measurement, which is fed to the DC-DC converter control system. It is observed from the simulation results, for the same load change, in an islanded single bus microgrid system, the deviation of bus frequency from its nominal value is less when both the battery storage system and PV systems are operated in droop control compared to when battery storage system alone is operated in droop control. Hence, operating the PV system in droop control mode improves the frequency regulation of islanded microgrid system.

A comparative study of different LPPT control schemes is also presented with respect to a dual-stage grid-connected PV system. Three different LPPT control schemes are considered. Those are FSLPPT, VSLPPT and VRLPPT. It is found from the simulation results that VRLPPT control scheme is superior to other control schemes as it exhibits minimum oscillations and renders faster power tracking. Hence, by applying VRLPPT control scheme for extracting the desired amount of power from PV system as commanded by the droop controller results in improving the frequency regulation of an islanded microgrid and also the frequency oscillations are minimized in steady state.

5.2 Future Work

The scope of this approach can be summarized as

- i. Implementing the droop control operation of PV system for frequency regulation of multi-bus

islanded microgrid network.

- ii. Droop control operation of PV system for frequency regulation of grid connected network.
- iii. Developing LPPT control for PV system to work even under partially shaded conditions.

References

- [1] M. G. Villava, J. R. Gazoli, and E. R. Filho, "Comprehensive approach to modelling and simulation of photovoltaic arrays," *IEEE Trans. Power Electron.*, vol. 24, no. 5, pp. 1198-1208, May. 2009.
- [2] T. Eswam and P. L. Chapman, "Comparison of photovoltaic array maximum power point tracking techniques," *IEEE Trans. Energy Convers.*, vol. 22, no. 2, pp. 434-449, Jun. 2007.
- [3] S. Jain and V Agarwal, "Comparison of the performance of maximum power point tracking schemes applied to single-stage grid-connected photovoltaic systems," *IET Electric Power Applications.*, vol. 1, issue. 5, pp. 753-762, 2007.
- [4] A. Urtasun, P. Sanchis, and L. Marroyo, "Limiting the power generated by photovoltaic system," in *Proc. Int. Multi-Conf. Syst. Signals and Devices.*, Mar. 2013, pp. 1-6.
- [5] P. B. S. Kiran and Vaskar Sarkar, "Improved limited power tracking of a photovoltaic plant connected across voltage-controlled DC bus," in *Proc. IEEE Ind. Commercial Power Syst./Petroleum and Chemical Ind. Conf. (ICPSPCIC).*, Nov. 2015.
- [6] J. A. Duffie and W. A. Beckman, *Solar Engineering of Thermal Processes.*, 2nd ed. New York: Wiley, 1991.
- [7] R. C. Neville, *Solar Energy Conversion: The Solar Cell.*, 2nd ed. New York: Elsevier, 1995.
- [8] J. A. Gow and C. D. Manning, "Development of a photovoltaic array model for use in power-electronics simulation studies," in *Proc. Inst. Elect. Eng., Elect. Power Appl.*, vol. 146, no. 2, pp. 193-200, 1999.
- [9] D. S. H. Chan and J. C. H. Phang, "Analytical methods for the extraction of solar-cell single- and double-diode model parameters from I-V characteristics," *IEEE Trans. Electron Devices.*, vol. ED-34, no. 2, pp. 286-293, Feb. 1987.
- [10] K. Nishioka, N. Sakitani, Y. Uraoka, and T. Fuyuki, "Analysis of multicrystalline silicon solar cells by modified 3-diode equivalent circuit model taking leakage current through periphery into consideration," *Solar Energy Mater. Solar Cells.*, vol. 91, no. 13, pp. 1222-1227, 2007.
- [11] N. Femia, G. Petrone, G. Spagnuolo, and M. Vitelli, "Optimization of perturb and observe maximum power point tracking method," *IEEE Transactions on Power Electronics.*, vol. 20, issue. 4, pp. 963-973, 2005.

- [12] A. K. Abdelsalam, A. M. Massoud, S. Ahmed, and P. N. Enjeti, "High-performance adaptive perturb and observe MPPT technique for photovoltaic-based microgrids," *IEEE Transactions on Power Electronics.*, vol. 26, issue. 4, pp. 1010-1021, 2011.
- [13] A. Safari and S. Mekhilef, "Simulation and hardware implementation of incremental conductance MPPT with direct control method using cuk converter," *IEEE Transactions on Industrial Electronics.*, vol. 58, issue. 4, pp. 1154-1161, 2011.
- [14] W. Xiao and W. G. Dunfort, "A modified adaptive hill climbing MPPT method for photovoltaic power systems," 35th Annual *IEEE Power Electronics Specialists Conference (PESC)*., vol. 3, pp. 1957-1963, 2004.
- [15] B. N. Alajmi, K. H. Ahmed, S. J. Finney, and B. W. Williams, "Fuzzy-Logic-Control approach of a modified hill-climbing method for maximum power point in microgrid standalone photovoltaic system," *IEEE Transactions on Power Electronics.*, vol. 26, issue. 4, pp. 1022-1030, 2011.
- [16] T. Esumi, J. W. Kimball, P. T. Krein, P. L. Chapman, and P. Midya, "Dynamic maximum power point tracking of photovoltaic arrays using ripple correlation control," *IEEE Transactions on Power Electronics.*, vol. 21, no. 5, pp. 1282-1291, 2006.
- [17] J.W. Kimball, P.T. Krein, "Discrete-Time ripple correlation control for maximum power point tracking," *IEEE Transactions on Power Electronics.*, vol. 23, no. 5, pp. 2353-2362, Sept. 2008.
- [18] P. B. S. Kiran, K. Manjunath, and V. Sarkar, "Limited power control of a single-stage grid connected photovoltaic system," in *Proc. IEEE Indian Conference (INDICON)*., Dec. 2015, pp. 1-6.
- [19] F. Liu, S. Duan, F. Liu, B. Liu, and Y. Kang, "A variable step size INC MPPT method for PV systems," *IEEE Trans. Ind. Applicat.*, vol. 55, no. 7, pp. 2622-2628, Jul. 2008.
- [20] [Online]. Available: <http://energystorage.org/energy-storage/technology-applications/frequency-regulation>.
- [21] M. B. Delghavi and A. Yazdani, "A control strategy for islanded operation of a distributed resource (DR) unit," in *Proc. IEEE Power Eng. Soc. General Meeting.*, Jul. 2009, pp. 26-30.
- [22] A. Yazdani and R. Iravani, *Voltage-Sourced Converters in Power Systems.*, Piscataway, NJ: IEEE/Wiley, 2010.